Acoustic field modeling in therapeutic ultrasound

T. Douglas Mast*, Waseem Faidi† and Inder Raj S. Makin†

*Department of Biomedical Engineering, University of Cincinnati, Cincinnati, Ohio 45267-0586
†Ethicon Endo-Surgery, 4545 Creek Rd., Cincinnati, Ohio 45242

Abstract. Understanding of ultrasound-tissue interaction is important for realization of clinically useful therapeutic ultrasound methods and devices. Linear acoustic propagation in homogeneous media, including diffraction and absorption effects, provides a useful first approximation but fails to accurately model many problems of interest. Depending on the therapy regime, other important effects can include finite-amplitude propagation, cavitation and other gas activity, inhomogeneous tissue structure, temperature-dependent tissue properties, and irreversible tissue modification. For bulk ablation of soft tissue using ultrasound, prediction of therapeutic effects requires accurate knowledge of space- and time-dependent heat deposition from acoustic absorption. A primary factor affecting heat deposition is local heat loss due to blood flow, both from bulk perfusion and large vessels. Gas activity due to boiling and tissue property changes due to local ablation, both of which markedly affect treatment, can be approximated by appropriate modification of the initial heat deposition pattern. Acoustically inhomogeneous tissue structure, even in nominally homogeneous organs such as the liver, can modify heating patterns enough to change treatment outcomes. These issues are illustrated by simulations of ultrasound therapy and comparison with *in vivo* and *in vitro* ultrasound ablation experiments.

Keywords: HIFU, intense ultrasound, ablation therapy, bio-heat transfer, numerical simulation.
PACS: 43.80.Sh, 43.58.Ta, 43.25.Jh

INTRODUCTION

Ablation of soft tissue using ultrasound has been investigated for a number of years [1] and is an active area of current engineering and medical research [2]. This paper reviews recent work on simulation of thermal therapy using numerical modeling of ultrasound propagation. Emphasis is given to modeling of bulk ablation using intense ultrasound beams that are unfocused or weakly focused; this approach has been developed for interstitial treatment of focal tumors [3]–[6].

Previous numerical studies of ultrasound ablation have provided insight into the dynamics of lesion formation in high-intensity focused ultrasound (HIFU) treatments, including the effects of blood flow cooling [7, 8], acoustic nonlinearity [8]–[12], cavitation [9], and thermoacoustic lensing effects [11, 12]. Modeling of interstitial ablation has also been performed, using numerical solution of the bioheat-transfer equation [13] with various methods for simulation of the ultrasound-induced heat deposition [4, 5, 14, 15]. Effects considered in these simulations have included loss of tissue perfusion and changes in ultrasound absorption due to thermal coagulation [5, 14, 15].

Here, methods for simulation of ultrasound therapy are briefly reviewed, and modeling of several propagation phenomena relevant to bulk ablation is described. For the therapy regime considered here, primary mechanisms altering ablation results include inhomogeneous cooling due to blood flow, distortion of therapy beams due to acousti-

CP838, *Innovations in Nonlinear Acoustics: 17th International Symposium on Nonlinear Acoustics*,
edited by A. A. Atchley, V. W. Sparrow, and R. M. Keolian

cally inhomogeneous tissue, and alteration of heat deposition due to tissue boiling, while finite-amplitude propagation and inertial cavitation are identified as secondary effects.

INTENSE ULTRASOUND ABLATION

Background

An approach for interstitial intense ultrasound ablation has been described elsewhere [6, 16]. In this concept, an ultrasound probe capable of both B-scan imaging and intense ultrasound ablation is inserted into target tissue, using a percutaneous, laparoscopic, or open-surgery approach. The probe is then used to image the target tissue, allowing user planning of an ablation procedure, and thermal ablation of a tissue volume is performed using electronic scanning and mechanical probe rotation.

A probe configuration suggested to be suitable for such an interstitial approach is an ultrasound array operating at a frequency 3.1 MHz, capable of acoustic energy densities > 80 W/cm^2 at the the probe surface, with active dimensions of about 2.3×49 mm^2 [6]. Construction of such arrays is feasible using an acoustic stack design that provides both high power capabilities for ablation and broad bandwidth for imaging [16]. Imaging and therapy performance for arrays of this type has been described recently [6].

Numerical modeling in homogeneous media

Simulation of ultrasound ablation requires a numerical model for propagating ultrasound, which acts as a heat source due to absorption. The Pennes bio-heat transfer equation, which represents heat diffusion with an added term for perfusion losses [13], can then be solved numerically, typically by finite-difference methods [15].

Typically, cumulative thermal damage to tissue is measured using the thermal dose [17], which is defined in units of equivalent minutes at 43°C. Typically assumed tissue damage thresholds, based on the thermal dose, are on the order of $\mathrm{EM}_{43} = 200$ min for cell death and $\mathrm{EM}_{43} = 10^7$ min for complete protein denaturation and severe coagulative necrosis [15]. These values correspond to measurable transitions in the ultrasonic absorption of soft tissue [18].

For absorption caused by relaxation processes, the rate of heat deposition per unit volume is $Q = \alpha|p|^2/(\rho c)$ [19], where α is the acoustic absorption in nepers per unit length, $|p|$ is the pressure amplitude of a time-harmonic acoustic field, and c is the speed of sound. Acoustic fields induced by ultrasound transducers can be simulated in a number of manners suitable for efficient numerical computations, including the Fresnel approximation for the fields of rectangular elements [6, 20], exact series solutions for disk radiators in unfocused [21, 22] and focused [23] configurations, and the KZK equation for approximations of finite-amplitude propagation [24, 25]. Acoustic absorption effects can be incorporated directly into any of these models, or can be applied *post hoc* in an approximate manner. The approximate approach to absorption modeling is convenient for representing changes in heat deposition due to tissue modification without further computation of the full acoustic field [15].

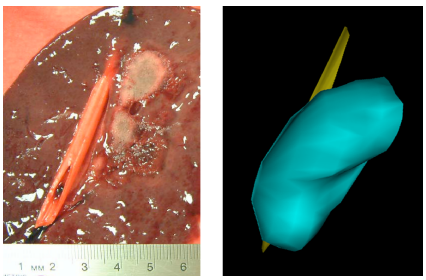

FIGURE 1. Lesion from an *in vivo* interstitial, rotationally scanned exposure, showing cooling effects caused by a large blood vessel. Left: cross section approximately along the probe track (thermally coagulated tissue is indicated by its lighter shade). Right: surface rendering of reconstructed lesion.

PHENOMENA AFFECTING ULTRASOUND ABLATION

Although numerical models of ultrasound ablation employing homogeneous media provide considerable insight, their results often disagree with real therapy results. In particular, such models fail to predict the significant variability of real ablation results *in vivo*. Below, several phenomena causing such discrepancies are discussed, with attention to methods for modeling these effects.

Inhomogeneous cooling

One of the most important factor affecting ultrasound ablation is the cooling caused by blood flow. The standard Pennes bio-heat equation, which incorporates cooling by a bulk perfusion term, is sufficient to explain many differences between ablation effects in excised tissue (*in vitro*) and in living systems (*in vivo*). However, cooling effects caused by large vessels can significantly alter local ablation results, potentially causing tissue near the blood vessels to remain untreated.

An example of this effect is illustrated in Fig. 1, which illustrates a thermal lesion induced in porcine liver *in vivo* by a scanned interstitial treatment. The treatment employed a 3.1 MHz, 3 mm diameter (2.3×49 mm^2 active surface) array firing with an acoustic power of 66.7 W (source intensity of 59.5 W/cm^2) and an 80% duty cycle, for four 1.5 min treatments at adjacent angles separated by 15°. In the vicinity of a large blood vessel, tissue ablation is substantially reduced due to local cooling effects. Numerical modeling of ablation in the presence of large blood vessels can be performed using appropriate boundary conditions for heat transfer at the vessel walls [8].

Acoustic nonlinearity and inertial cavitation

For the intense ultrasound beams employed in bulk ablation, finite-amplitude propagation has a nonzero effect, due to both waveform steepening (generation of higher

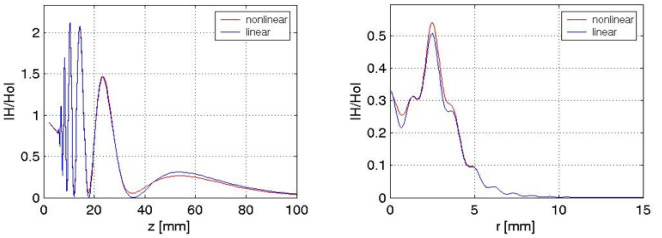

FIGURE 2. Estimated effects of acoustic nonlinearity on ultrasound heat deposition for a 12 mm, 3 MHz disk radiating at 1.5 MPa into liver tissue. The plots show the squared pressure amplitude for a linear computation together with the squared amplitude (summed over all computed harmonics) for a fully nonlinear solution of the KZK equation. Left: squared amplitude along the transducer axis. Right: squared amplitude as a function of azimuth at a distance of 30 mm from the transducer face.

harmonics) and inertial cavitation. Previous models have illustrated the effects of acoustic nonlinearity [8]–[12] and cavitation [9] on HIFU treatments.

For the ultrasound bulk ablation configuration described above, a typical acoustic pressure amplitude is about 1.5 MPa at the transducer surface, corresponding to an energy density of about 70 W/cm^2. An example computation illustrating the effects of acoustic nonlinearity on heat deposition employs a numerical solution to the KZK equation [24, 25] for a disk of diameter 12 mm (area similar to a rectangular aperture of dimensions 2.3×49 mm^2) radiating at 3 MHz with an amplitude of 1.5 MPa into a medium with acoustic properties comparable to human liver ($c = 1540$ m/s, $\rho = 1060$ kg/m^3, $\alpha = 5.75$ Np/cm/MHz$^{1.2}$, and nonlinearity coefficient $\beta = 4.7$). For these parameters, the resulting squared pressure amplitude (proportional to heat deposition) is illustrated in Fig. 2. A fully nonlinear computation is shown to cause heat deposition that varies only slightly from the linear case. Thus, in this case acoustic nonlinearity does not have a great effect on ablation results, compared to other phenomena described here.

The importance of inertial cavitation can be assessed using the mechanical index (MI) [26], defined as the maximum rarefaction pressure in MPa divided by the square root of the frequency in MHz. For an amplitude of 1.5 MPa and a frequency of 3 MHz, the MI is 0.866, and this value decreases further with depth, due to acoustic absorption. As this value is substantially less than the maximum value of 1.9 generally recognized as safe for diagnostic ultrasound, it may be assumed that inertial cavitation is a relatively minor effect in bulk ablation using unfocused intense ultrasound beams.

Inhomogeneous propagation

Most simulations of ultrasound propagation for therapy modeling have assumed tissue structure either to be uniform [8, 15] or composed of uniform layers [11]. However, the inhomogeneous structure of real tissue, which causes distortion of ultrasound beams known to cause significant aberration in ultrasound imaging [29], is equally relevant to ultrasound therapy.

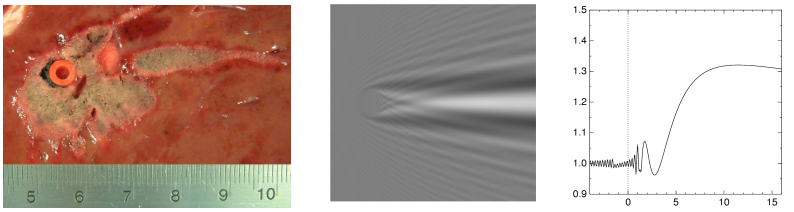

FIGURE 3. Acoustic effects of a large blood vessel on interstitial bulk ablation. Left: cross section of a thermal lesion created *in vivo* with a rotationally scanned 3 mm, 3.1 MHz array, showing anomalously large ablation distal to the vessel. Center: total squared pressure amplitude, relative to the plane wave amplitude, for a 3.1 MHz plane wave scattered by a 3 mm blood-mimicking cylinder in a liver-mimicking background, plotted on a linear gray scale. Right: squared pressure along the axis of symmetry for the same simulation.

In a common noninvasive HIFU configuration, a highly focused ultrasound beam propagates through the abdominal wall to ablate tissue in the abdominal cavity, such as a liver tumor [27, 28]. Measurements [29] and simulations [30] have indicated that propagation through the abdominal wall can cause random fluctuations on the order of 3 dB (rms) in the transmitted amplitude, due both to scattering and inhomogeneous absorption. A 3 dB change in amplitude, which corresponds to a factor of two in heat deposition, causes the time required for local tissue ablation to be correspondingly changed by a factor of two, large enough to significantly change ablation results for a given treatment plan.

In nominally homogeneous organs such as the liver, inhomogeneous tissue structure can still affect ablation results. An example from an interstitial ablation experiment performed *in vivo* in porcine liver is shown in Fig. 3. In this case, anomalously severe and deep ablation occurred distal to a large blood vessel. A plausible explanation for this result is acoustic focusing caused by the difference in sound speed between blood and liver parenchyma. To illustrate this explanation, a computation performed using the exact solution for scattering from a fluid cylinder [31] is also shown in Fig. 3. In this computation, the liver background was modeled as a fluid with sound speed 1595 m/s and the blood vessel was modeled as a cylinder with sound speed 1580 m/s. The results show substantial focusing resulting in over a 50% increase in peak heat deposition, consistent with the increased lesioning shown.

More general computations of propagation in inhomogeneous tissue for therapy modeling can be performed using three-dimensional tissue models, which can be established from image data such as cross-sectional photography or volumetric CT scans [32, 33]. For large-scale three-dimensional computations, such as those required for simulation of ultrasound therapy, a particularly useful approach is the *k*-space method [34, 35], which provides accurate results for relatively coarse spatial and temporal discretization. This method has been extended to incorporate perfectly-matched-layer absorbing boundary conditions and tissue absorption caused by relaxation processes [36]. Recent applications have included 3D simulations of propagation in breast tissue [33], simulations of focus distortion in large-scale 2D tissue models [37], and computations of propagation in a 3D prostate tissue model for simulation of ultrasonic hyperthermia [38].

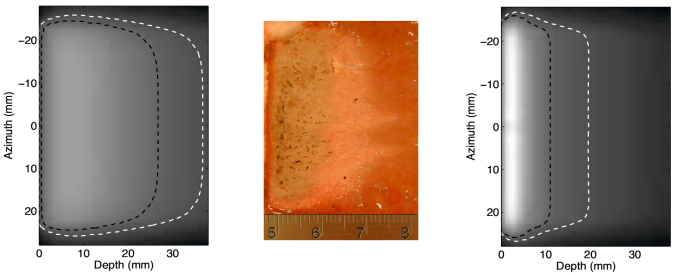

FIGURE 4. Effect of boiling and thermal dose dependent attenuation. Left: simulation without boiling and dose-dependent attenuation modeling. The simulated thermal dose is shown on a logarithmic gray scale with superimposed contours at EM_{43}=200 and 10^7 equivalent minutes. Center: *In vitro* lesion. Right: simulated thermal dose with boiling and dose-dependent attenuation modeling.

Tissue modification

Particularly severe effects on ultrasound ablation are caused by changes to tissue acoustic properties that result from thermal coagulation. These include increases in tissue absorption that have been quantified by measurements [18] and gas activity due to tissue boiling, which has been observed to alter positions and extents of HIFU lesions [39, 40]. Recent numerical models for bulk ultrasound ablation have incorporated both of these effects.

Changes in tissue absorption associated with ablation can be incorporated based on the thermal dose, in correspondence with measurements [18]. Some models have assigned a single increased absorption value to all tissue locations that have surpassed a thermal dose threshold [5]. In order to better match measurements, other models have incorporated a linear rise in absorption above a thermal dose threshold on the order of $EM_{43} = 200$ min, with a maximum set by a second thermal dose threshold on the order of $EM_{43} = 10^7$ min [14, 15].

The effects of tissue boiling, which include both strong shadowing and increased local absorption, can limit the achievable depth of ultrasound ablation. This effect has been modeled for single HIFU lesions by assuming that, after any grid point (usually near the acoustic focus) reached a temperature of 100°C, all of the thermal energy originally deposited in the distal half-space was redistributed in a 0.5 cm spherical region centered around the initial location of tissue boiling [10]. For simulation of bulk tissue ablation, in which boiling effects are not necessarily localized at a focal point, this idea has been extended to more general heat distributions [15]. In the more general approach, the thermal energy deposited within the distal region projected (shadowed) by all boiling points is equally distributed around each of the proximal grid points where the temperature has exceeded 100°C.

These tissue modification effects can substantially effect ultrasound bulk ablation, as illustrated by Fig. 4. The lesion shown was created *in vitro* in porcine liver tissue by a 3 mm, 3.1 MHz array firing for 3 min with a surface power density of 39 W/cm^2 and an 80% duty cycle. The simulated thermal dose maps shown were obtained by identical

methods except for consideration of boiling and thermal dose-dependent attenuation [15]. The simulation incorporating these tissue modification effects agrees much better with the experimental result for the depth, overall shape, and rate of thermal ablation.

CONCLUSIONS

Modeling of therapeutic ultrasound requires consideration of an array of potential complicating effects. For interstitial bulk ablation, the most important effects include the thermal and acoustic effects of natural tissue inhomogeneities as well as tissue changes caused by the therapy itself. Other therapy regimes can require different considerations for accurate modeling, such as explicit treatment of finite-amplitude propagation and inertial cavitation. For any form of ultrasound therapy, it is likely that natural variations of tissue properties and structure will limit the predictive accuracy of simulations. Thus, methods for accurate monitoring and assessment of ultrasound ablation effects could increase the clinical viability of therapeutic ultrasound.

REFERENCES

1. W. J. Fry, "Biological and medical acoustics," J. Acoust. Soc. Am. **30**, 387–393 (1958).
2. J. E. Kennedy, G. R. ter Haar, and D. Cranston, "High intensity focused ultrasound: surgery of the future?" Br. J. Radiol. **76**, 590–599 (2003).
3. C. J. Diederich, W. H. Nau, and P. R. Stauffer, "Ultrasound applicators for interstitial thermal coagulation," IEEE Trans. Ultras., Ferroelect., Freq. Contr. **46**, 1218–1228 (1999).
4. R. Chopra, M. J. Bronskill, and F. S. Foster, "Feasibility of linear arrays for interstitial ultrasound thermal therapy," Med. Phys. **27**, 1281–1286 (2000).
5. C. Lafon, F. Prat, J. Y. Chapelon, F. Gorry, J. Margonari, Y. Theillere, and D. Cathignol, "Cylindrical thermal coagulation necrosis using an interstitial applicator with a plane ultrasonic transducer: *in vitro* and *in vivo* experiments versus computer simulations," Int. J. Hyperthermia **16**:508–522 (2000).
6. I. R. S. Makin, T. D. Mast, W. Faidi, M. M. Runk, P. G. Barthe, and M. H. Slayton, "Miniaturized ultrasound arrays for interstitial ablation and imaging," Ultras. Med. Biol., to appear (2005).
7. M. C. Kolios, M. D. Sherar, and J. W. Hunt, "Blood flow cooling and ultrasonic lesion formation," Med. Phys. **23**, 1287–1298 (1996).
8. F. P. Curra, P. D. Mourad, V. A. Khoklova, R. O. Cleveland, and L. A. Crum, "Numerical simulations of heating patterns and tissue temperature response due to high-intensity focused ultrasound," IEEE Trans. Ultras., Ferroelect., Freq. Contr. **47**, 1077–1089 (1999).
9. F. Chavrier, J. Y. Chapelon, A. Gelet, and D. Cathignol, "Modeling of high-intensity focused ultrasound-induced lesions in the presence of cavitation bubbles," J. Acoust. Soc. Am. **108**, 432–440 (2000).
10. P. M. Meaney, M. D. Cahill, and G. R. ter Haar, "The intensity dependence of lesion position shift during focused ultrasound surgery," Ultras. Med. Biol. **26**, 441–450 (2000).
11. I. M. Hallaj, R. O. Cleveland, and K. Hynynen, "Simulations of the thermo-acoustic lens effect during focused ultrasound surgery," J. Acoust. Soc. Am. **109**, 2245–2253 (2001).
12. C. W. Connor and K. Hynynen, "Bio-acoustic thermal lensing and nonlinear propagation in focused ultrasound surgery using large focal spots: a parametric study," Phys. Med. Biol. **47**, 1911–1928 (2002).
13. H. H. Pennes, "Analysis of tissue and arterial blood temperatures in the resting human forearm," J. Appl. Physiol. **1**, 93–122 (1948).
14. P. D. Tyreus and C. J. Diederich, "Theoretical model of internally cooled interstitial ultrasound applicators for thermal therapy," Phys. Med. Biol. **47**:1073–1089 (2002).

15. T. D. Mast, I. R. S. Makin, W. Faidi, M. M. Runk, P. G. Barthe, and M. H. Slayton, "Bulk ablation of soft tissue with intense ultrasound: modeling and experiments," J. Acoust. Soc. Am., to appear (2005).
16. P. G. Barthe and M. H. Slayton, "Efficient wideband linear arrays for imaging and therapy," 1999 IEEE Ultrasonics Symposium Proceedings, Vol. 2, pp. 1249–1252.
17. S. A. Sapareto and W. C. Dewey, "Thermal dose determination in cancer therapy," Int. J. Radiat. Oncol. Biol. Phys. **10**, 787–800 (1984).
18. C. A. Damianou, N. T. Sanghvi, F. J. Fry, and R. Maass-Moreno, "Dependence of ultrasonic attenuation and absorption in dog soft tissues on temperature and thermal dose," J. Acoust. Soc. Am. **102**, 628–634 (1997).
19. W. L. Nyborg, "Heat generation by ultrasound in a relaxing medium," J. Acoust. Soc. Am. **70**, 310–312 (1981).
20. A. Freedman, "Sound field of a rectangular piston," J. Acoust. Soc. Am. **32**, 197–209 (1960).
21. T. Hasegawa, N. Inoue, and K. Matsuzawa, "Fresnel diffraction: Some extensions of the theory," J. Acoust. Soc. Am. **75**, 1048–1051 (1984).
22. T. D. Mast and F. Yu, "Simplified expansions for radiation from a baffled circular piston," J. Acoust. Soc. Am., submitted (2005).
23. T. Hasegawa, N. Inoue, and K. Matsuzawa, "A new theory for the radiation from a concave piston source," J. Acoust. Soc. Am. **82**, 706–708 (1987).
24. E. A. Zabolotskaya and R. V. Khokhlov, "Quasi-plane waves in the non-linear acoustics of confined beams," Sov. Phys. Acoust. **15**, 35–40 (1969).
25. V. P. Kuznetsov, "Equation of nonlinear acoustics," Sov. Phys. Acoust. **16**, 467–470 (1970).
26. R. E. Apfel and C. K. Holland, "Gauging the likelihood of cavitation from short-pulse, low duty cycle diagnostic ultrasound," Ultrasound Med Biol. **17**, 179–185 (1991).
27. G. R. ter Haar, D. Sinnett, and I. Rivens, "High-intensity-focused ultrasound: a surgical technique for the treatment of discrete liver tumors," Phys. Med. Biol. **34**, 1743–1750 (1989).
28. F. Wu, W.-Z. Chen, J. Bai, J.-Z. Zou, Z.-L. Wang, H. Zhu, and Z.-B. Wang, "Pathological changes in human malignant carcinoma treated with high-intensity focused ultrasound," Ultras. Med. Biol. **27**, 1099–1106 (2001).
29. L. M. Hinkelman, T. D. Mast, L. A. Metlay, and R. C. Waag, "The effect of abdominal wall morphology on ultrasonic pulse distortion. Part I: Measurements." J. Acoust. Soc. Am. **104**:3635–3649 (1998).
30. T. D. Mast, L. M. Hinkelman, M. J. Orr, V. W. Sparrow, and R. C. Waag, "Simulation of ultrasonic propagation through the abdominal wall," J. Acoust. Soc. Am. **102**, 1177–1190 (1997).
31. P. M. Morse and K. U. Ingard, *Theoretical Acoustics* (McGraw-Hill, New York, 1968), Ch. 8.
32. J. L. Aroyan, "Three-dimensional modeling of hearing in *Delphinus delphis*," J. Acoust. Soc. Am. **110**, 3305–3318 (2001).
33. T. D. Mast, "Two- and three-dimensional simulations of ultrasonic propagation through human breast tissue," Acoust. Res. Lett. Online **3**, 53–58 (2002).
34. N. N. Bojarski, "The *k*-space formulation of the scattering problem in the time domain: an improved single propagator formulation," J. Acoust. Soc. Am. **77**, 826–831 (1985).
35. T. D. Mast, L. P. Souriau, D.-L. Liu, M. Tabei, A. I. Nachman, and R. C. Waag, "A *k*-space method for large-scale models of wave propagation in tissue," IEEE Trans. Ultrason., Ferroelectr., Freq. Contr. **48**, 341–354 (2001).
36. M. Tabei, T. D. Mast, and R. C. Waag, "A *k*-space method for coupled first-order acoustic propagation equations," J. Acoust. Soc. Am. **111**, 53–63 (2002).
37. M. Tabei, T. D. Mast, and R. C. Waag, "Simulation of ultrasonic focus aberration through human tissue," J. Acoust. Soc. Am. **113**, 1166–1176 (2003).
38. O. M. Al-Bataineh, N. B. Smith, R. M. Keolian, V. W. Sparrow, and L. E. Harpster, "Optimized hyperthermia treatment of prostate cancer using a novel intracavitary ultrasound array," J. Acoust. Soc. Am. **114**, 2347 (2003).
39. N. A. Watkin, G. R. ter Haar, and I. Rivens, "The intensity dependence of the site of maximal energy deposition in focused ultrasound surgery," Ultras. Med. Biol. **22**, 483–491 (1996).
40. W.-S. Chen, C. Lafon, T. J. Matula, S. Vaezy, and L. A. Crum, "Mechanisms of lesion formation in high intensity focused ultrasound therapy," Acoust. Res. Lett. Online **4**, 41–46 (2003).